

High dimensional discriminant rules with shrinkage estimators of the covariance matrix and mean vector

Jaehoan Kim*, Junyong Park[†] and Hoyoung Park[‡]

November 2022

Abstract

Linear discriminant analysis (LDA) is a typical method for classification problems with large dimensions and small samples. There are various types of LDA methods that are based on the different types of estimators for the covariance matrices and mean vectors. In this paper, we consider shrinkage methods based on a non-parametric approach. For the precision matrix, methods based on the sparsity structure or data splitting are examined. Regarding the estimation of mean vectors, Non-parametric Empirical Bayes (NPEB) methods and Non-parametric Maximum Likelihood Estimation (NPMLE) methods, also known as f -modeling and g -modeling, respectively, are adopted. The performance of linear discriminant rules based on combined estimation strategies of the covariance matrix and mean vectors are analyzed in this study. Particularly, the study presents a theoretical result on the performance of the NPEB method and compares it with previous studies. Simulation studies with various covariance matrices and mean vector structures are conducted to evaluate the methods discussed in this paper. Furthermore, real data examples such as gene expressions and EEG data are also presented.

*Department of Statistics, Texas A&M University, TX, USA, k1mjh6561@tamu.edu

[†]Department of Statistics, Seoul National University, Seoul, Korea, junyongpark@snu.ac.kr

[‡]Department of Statistics, Sookmyung Women's University, Seoul, Korea, hyparks@sookmyung.ac.kr

Keywords : High dimensional discriminant analysis; Nonparametric maximum likelihood estimation; Nonparametric empirical Bayes; Estimation of precision matrix

1 Introduction

Discriminant analysis is one of the most widely emerging problems in various fields, including marketing, biomedical studies, sociology, and psychology. Due to the development of data collection technology, the data which contains the larger number of features than the number of samples became prevalent. Therefore, discriminant analysis in high-dimensional situations became important. Owing to its simplicity and optimality under the knowledge of parameters (see [1]), the Fisher's linear discriminant analysis (LDA) received a lot of attention and has been studied intensively in both theory and practical applications. Since this linear discriminant rule requires mean vectors and the precision matrix, they should be estimated in practical situations. However, especially for high dimensional situations, precision matrix should be estimated carefully. Since the sample covariance matrix is not invertible anymore, the inverse of the sample covariance matrix is no more valid as an estimator. Therefore, there have been numerous studies to resolve this problem and construct the linear discriminant rules.

First, there were several approaches to estimating the precision matrix as a diagonal one, by simply assuming the independence among features. Since this assumption makes the true covariance matrix to be diagonal, it only requires each feature's precision to be estimated. The discriminant rule based on this assumption is called the independence rule (IR). In addition to that, feature selection had been added on this assumption with intuition to "reduce the noise from data". This led to the feature annealed independence rule (FAIR), studied in [8], showing that the FAIR method can improve the error rate of the IR method in real data situations.

However, the IR and the FAIR are restrictive since they ignore all the possible dependence among features, which might be crucial if there exist some features which are crucially related, for example, voxels in fMRI data. Therefore, there have been several approaches to preserve

the ‘structure’, which also can be considered as connectivity, of original data.

One possible approach is to slightly modify the sample covariance matrix into an invertible form using the idea of a shrinkage estimator. For the sample covariance matrix S and $0 < \lambda < 1$, one can take $S' = (1 - \lambda)S + \lambda I$ as the covariance estimator and use its inverse as the estimator of the precision matrix. In addition, other approaches of precision estimation are proposed to solve the optimization problem with penalty terms. See [4] and [9] for more detailed explanations. [14] suggested nonparametric sample splitting technique for the estimation.

There is some research on utilizing these estimators of covariance or precision matrix in high dimensional discriminant analysis. For example, [16] presented intensive comparisons among discriminant rules based on various estimators of covariance or precision matrix. It is shown that the non-parametric mean vector estimation method and the precision estimator proposed in [14] provided the best overall performance. Although [16] presented various results, some important methodologies are missing. For example, mean vector estimation based on the NPEB in [10] has not been considered in their study and the sparse precision matrix has not been combined with such mean vector estimations, either.

In addition to the estimation of covariance or precision matrix, mean vector estimation has several approaches as well. For the general mean estimation approach, [7] categorized estimation strategies in empirical Bayes into the f -modeling and g -modeling which had been actually used in many estimation problems before. There are several attempts to utilize these strategies into discriminant analysis problem. See [10] and [6] for f -modeling and [5] and [16] for g -modeling in high dimensional discriminant analysis. The theoretical properties of the discriminant rules based on these estimators are gradually unveiled especially for g -modelling rather than f -modelling; see [5] and [17] for theoretical studies on the discriminant rule based on g -modelling. Although [10] and [6] used the f -modelling, to the best of our knowledge, there has been no study on theoretical properties of high dimensional discriminant rule based on f -modelling for estimating mean vectors. It is worth noting that both f -modelling and g -modeeling in mean vector estimations assume independence among features, which requires

appropriate data decorrelation before applying these strategies.

In this context, our paper displays two main extensions. First, we elaborate on the impact of the aforementioned estimation methods for precision matrices and mean vectors on the constructed discriminant rules. Since mean vector estimation methods require the precision matrix to remove the dependency in the data before applied, the effect of the two estimators is intertwined. Hence, we cross check the estimation method, we analyze the impact of the estimators on real data examples. Second, we newly analyze the theoretical property of the discriminant rule based on the f-modeling mean vector estimator. With the knowledge about the precision matrix, we consider the asymptotic situation in which the number of features diverges to infinity and compare this rule's asymptotic properties with others.

This paper is organized as follows. In section 2, we review the Fisher's rule and estimation of the covariance matrix and mean vector. In section 3, we provide the asymptotic results for nonparametric empirical Bayes method and comparison with other methods. Section 4 includes simulations studies to evaluate all the discriminant rules considered in this paper for various combinations of mean vectors and covariance matrices. In section 5, real data examples are also presented to compare all the discriminant rules. We summarize all the results in section 6 as concluding remarks.

2 Construction of discriminant rules

In this section, we review the methods of estimating precision matrix and mean vector in high dimensions. Throughout this paper, we assume $\mathbf{X}_{ij} \sim N_p(\boldsymbol{\mu}_i, \Sigma)$ for $i = 1, 2$ and $j = 1, \dots, n_i$. To avoid confusion, we use bold symbols to indicate vectors in this section.

A well-known linear discriminant rule, Fisher's linear discriminant analysis (LDA), can be written as

$$f(\mathbf{x}^{new}) = \frac{1}{2} [3 - \text{sign} \{\delta(\mathbf{x}^{new})\}]$$

for the new data $\mathbf{x}^{new} \in \mathbb{R}^p$, where

$$\delta(\mathbf{x}^{new}) = \left(\mathbf{x}^{new} - \frac{\boldsymbol{\mu}_1 + \boldsymbol{\mu}_2}{2} \right)^\top \Sigma^{-1} (\boldsymbol{\mu}_1 - \boldsymbol{\mu}_2). \quad (1)$$

$\delta(\mathbf{x}^{new})$ has the value 1 or 2 to indicate the group which the new observation is categorized. As one can see, Fisher's LDA requests two estimates, for $\boldsymbol{\mu}_i$ and $\Omega = \Sigma^{-1}$.

First, when estimating Ω , difficulty arises in high-dimensional situations since one cannot directly plug in the inverse of the sample covariance matrix due to its rank deficiency. Therefore, several alternatives exist to estimate Ω directly in high-dimensional situations. In this paper, we utilized the precision estimation methods using 1) L^1 penalty of the precision matrix (which is called the graphical Lasso method; we call this method 'glasso' in this paper; see [9]), and, 2) random sample splitting (we call this method 'LAM'; see [14]). Of course, we can assume the precision matrix to be diagonal and naively estimate each element. We write this method as 'IR,' which is the shorthand for 'Independence Rule'.

Regarding the estimation of $\boldsymbol{\mu}_i$, we use two methods based on two types of nonparametric empirical Bayes estimations, namely g -modeling and f -modeling introduced in [7]. Such mean vector estimations have been used in [10] and [5] under the independent assumption of variables. Obviously, we also consider the sample mean as an estimate of $\boldsymbol{\mu}_i$.

The mainstream of this paper is to examine the performance of different types of discriminant rules in high-dimensional situations and analyze their performance both practically and theoretically.

As a building block, we define the decorrelated observation \mathbf{Z}_{ij} as

$$\mathbf{Z}_{ij} = \Omega^{1/2} \mathbf{X}_{ij} \sim N(\Omega^{1/2} \boldsymbol{\mu}_i, I_p) \equiv N_p(\boldsymbol{\mu}_i^*, I_p) \quad (2)$$

where I_p is $p \times p$ identity matrix. Based on \mathbf{Z}_{ij} , the Fisher's rule is expressed as follows:

$$\begin{aligned}
\delta(\mathbf{x}^{new}) &= \left(\mathbf{x}^{new} - \frac{\boldsymbol{\mu}_1 + \boldsymbol{\mu}_2}{2} \right)^\top \Sigma^{-1} (\boldsymbol{\mu}_1 - \boldsymbol{\mu}_2) \\
&= \left\{ \Sigma^{-1/2} (\boldsymbol{\mu}_1 - \boldsymbol{\mu}_2) \right\}^\top \Sigma^{-1/2} \left(\mathbf{x}^{new} - \frac{\boldsymbol{\mu}_1 + \boldsymbol{\mu}_2}{2} \right)^\top \\
&= (\boldsymbol{\mu}_1^* - \boldsymbol{\mu}_2^*)^\top \left(\mathbf{z}^{new} - \frac{\boldsymbol{\mu}_1^* + \boldsymbol{\mu}_2^*}{2} \right) \\
&\equiv \sum_{i=1}^p a_i z_i^{new} + a_0
\end{aligned} \tag{3}$$

where $\mathbf{z}^{new} = \Omega^{1/2} \mathbf{x}^{new} = \Sigma^{-1/2} \mathbf{x}^{new}$, $a_i = \mu_{1i}^* - \mu_{2i}^*$ and $a_0 = -(\boldsymbol{\mu}_1^* - \boldsymbol{\mu}_2^*)^\top (\boldsymbol{\mu}_1^* + \boldsymbol{\mu}_2^*) / 2$. z_i^{new} denotes the i -th component of \mathbf{z}^{new} .

In practice, of course, $\Omega = \Sigma^{-1}$ is unknown, so we need to estimate $\hat{\Omega}$ and decorrelate \mathbf{X}_{ij} with $\hat{\Omega}^{1/2}$. If such estimates are accurate, one can expect that all variables in \mathbf{Z}_{ij} are nearly independent, hence we can apply the mean estimation methods described later, which assumes the independence of variables.

To summarize, we need two estimates to construct Fisher's discriminant rule: one for Ω (or Σ) and the other one for $\boldsymbol{\mu}_i$ (or $\boldsymbol{\mu}_i^*$). We present these two procedures in the following sections.

2.1 Estimation of precision matrix

In the case of the precision matrix estimation, we present two approaches: one is based on some special structural assumption, and the other one is for the general cases without this assumption. For the former case, it is widely assumed that the precision matrix has sparsity (relatively small number of nonzero components within the matrix) or graphical structure, as [4] and [9]. However, this structural assumption has limitations to be applied for general multivariate data. On the other hand, the latter case can be generally utilized since it is free of any structural assumption. See, for example, [14]. However, the data dimension gives a computational restriction compared to the former case. In this paper, we consider

the method based on the graphical model, called glasso in [9] as an example of the first approach. For the latter approach, we introduce the method based on random sample data splitting, called the LAM method in [14].

First, as previously mentioned, the glasso method is initially devised to estimate the precision matrix under the sparsity assumption. To utilize this assumption, [9] converted this estimation problem into the optimization problem, maximizing a penalized log-likelihood function with respect to the matrix Θ . The penalty term is given in the L_1 -norm of the precision matrix, which can favor the sparsity assumption. The objective function in glasso is written as

$$f(\Theta) = \log \det(\Theta) - \text{tr}(S_n \Theta) - \rho \|\Theta\|_1 \quad (4)$$

where S_n is sample covariance matrix, $\det(\Theta)$ is the determinant of Θ and ρ is the regularization parameter. The optimal value $\Theta^* = \text{argmax}_{\Theta} f(\Theta)$ is used as the estimator of Ω .

Subsequently, the LAM algorithm uses a random sample splitting idea. The fundamental issue for high dimensional data is that S_n is not invertible, which hinders S_n^{-1} to be used as an estimator for the precision matrix. To detour this problem, [14] applied the following strategy to construct an invertible estimator for the covariance matrix.

First, the true covariance matrix Σ can be represented as

$$\Sigma = PDP^T, D \succeq 0, \quad (5)$$

where P is the orthogonal matrix and D diagonal matrix. This can be also written as

$$\Sigma = PDP^T = P \text{diag}(P^T \Sigma P) P^T, \quad (6)$$

where $\text{diag}(A)$ denotes the diagonal matrix with diagonal elements of A . Based on this, to construct an invertible estimator $\hat{\Sigma}$ for Σ , [14] first split n observations into two groups of n_1 and $n_2 = n - n_1$ observations. Then, they used one group to estimate P and the other to estimate Σ for $\text{diag}(P^T \Sigma P)$. Since we already have two groups of observations, we can

use the first group of observations to estimate P , and the second group of n_2 observations to estimate Σ on the right-hand side of (6). Therefore, when we denote the sample covariance matrix of two groups as $S_{n,1}$, $S_{n,2}$, and \hat{P}_1 the eigenvectors of $S_{n,1}$, the estimator is represented as

$$\hat{\Sigma}_{LAM} = \hat{P}_1 \text{diag}(\hat{P}_1^T S_{n,2} \hat{P}_1) \hat{P}_1^T. \quad (7)$$

2.2 Estimation of mean vector

Estimation of the mean vector is another important component of Fisher LDA. In many cases, the estimation of the covariance matrix has been focused on high-dimensional discriminant analysis, and the sample means vector has been commonly used. Shrinkage estimator of the mean vector in high dimensional classification has been seriously considered under the assumption that the covariance matrix is a diagonal matrix, which is a modified form of the naive Bayes rule. [10] and [5] are representative work applying f -modeling and g -modeling to discriminant analysis under the assumption that all variables are independent.

When we have independent random variables $Y_i \sim N(\mu_i, 1)$ for $1 \leq i \leq p$, a lot of research has been done on the simultaneous estimation of the mean vector, $\boldsymbol{\mu} = (\mu_1, \dots, \mu_p)$. A typical example is the James-Stein estimator, but from a Bayesian point of view, it is an estimator under the assumption that each mean value is generated from a normal distribution, so it has the disadvantage of not reflecting the various structures of the mean values such as bi-modality of mean values which may occur for the case of the sparsity of mean values. When p is large, there are two typical methods in nonparametric empirical Bayes methods discussed in [7] : f -modeling based on the estimation of marginal density and g -modeling based on the estimation of mixing distribution or prior distribution as a non-parametric method. The detail of these two methods are discussed shortly. In particular, f -modeling has a simpler calculation process than g -modeling, however with the recent development of various algorithms that can be used for g -modeling, empirical Bayesian methods based on g -modeling are also widely used.

In fact, when estimating the mean vector via these methods, the observed values are assumed to be independent. However, in classification, this assumption is not satisfied in general. Although there exist correlations among all variables, existing studies such as [10] applied f -modeling method to correlated variables in high dimensional classification problems. Instead, since we can obtain an estimate of the precision matrix following the previous section, we can remove the correlation among the variables using the square root matrix of this obtained estimate.

More specifically, consider $\mathbf{X}_i \sim N_p(\boldsymbol{\mu}, \Sigma)$ with $i = 1, \dots, n$ and $p \times p$ positive definite matrix $\Omega^{1/2}$ where $\Omega = \Sigma^{-1}$. We consider the random variables \mathbf{Z}_i as follows:

$$\mathbf{Z}_i \equiv \Omega^{1/2} \mathbf{X}_i \sim N_p(\Omega^{1/2} \boldsymbol{\mu}, I_p) \equiv N_p(\boldsymbol{\mu}^*, I_p), \quad (8)$$

where $\boldsymbol{\mu} = (\mu_1, \dots, \mu_p)^T$, $\boldsymbol{\mu}^* = (\mu_1^*, \dots, \mu_p^*)^T$, $\mathbf{X}_i = (X_{i1}, \dots, X_{ip})^T$ and $\mathbf{Z}_i = (Z_{i1}, \dots, Z_{ip})^T$. Therefore, the j -th component of \mathbf{Z}_i , Z_{ij} , satisfies $Z_{ij} \sim N(\mu_j^*, 1)$ and is independently distributed. We estimate the mean vector $\boldsymbol{\mu}_i^*$ based on decorrelated observations $\mathbf{Z}_i = (Z_{i1}, \dots, Z_{ip})^T$ and then transform back to $\hat{\boldsymbol{\mu}}_i = R^{-1} \boldsymbol{\mu}_i^*$, aligned with the assumption of f -modeling and g -modeling.

Now we provide f - and g -modeling based estimation methods in detail. We consider one dimensional random variable Z and its observed value z_1, \dots, z_n , under the hierarchical structure

$$Z_i \sim N(\mu_i, 1), \quad \mu_i \sim G. \quad (9)$$

Here, G is a cumulative distribution function of μ . Under the Bayesian scheme, the probability distribution function of Z , g^* , is written as

$$g^*(z) = \int \phi(z - v) dG(v), \quad (10)$$

where $\phi(\cdot)$ is the probability distribution function of standard normal distribution, say $\phi(x) = \exp(-x^2/2)/\sqrt{2\pi}$. Under this structure, the Bayes estimator for μ_i is

$$E(\mu_i|z_i) = z_i + \frac{(g^*)'(z_i)}{g^*(z_i)}, \quad (11)$$

where $(g^*)'(z) = dg^*(z)/dz$.

There are two categories of estimator for $E(\mu_i|z_i)$: First one is $\widehat{g^*(z)} = \int \phi(z-v)d\hat{G}(v)$ with an estimator for G , called g -modeling. See [12] and [7]. The other one is estimating g^* directly by using density estimation based on the observed values z_1, \dots, z_p , called f -modeling. See [10]. We denote the first method as ‘NPMLE’ since we would estimate G with maximum likelihood estimator (MLE), and the latter one as ‘NPEB’.

To begin with, the NPMLE method requires G to be estimated and MLE can be used as the solution of the optimization problem

$$\hat{G} = \operatorname{argmax}_{F \in \mathcal{F}} \sum_{i=1}^n \log \left\{ \int \phi(z_i - \mu) dF(\mu) \right\}, \quad (12)$$

where \mathcal{F} is a set of distribution functions. It cannot be solved in its original form since \mathcal{F} is infinite-dimensional. Therefore, we must constrain this as a finite-dimensional one. [13] restricted \mathcal{F} into the set of piecewise constant distribution functions with $K+1$ regular grid points and converted this problem into K dimensional convex optimization problem. See [5] for details. The well-performing behavior of \hat{G} via this algorithm, even with a relatively small number of K ($K \approx \sqrt{n}$), is justified in [5]. This algorithm can be implemented in R via `REBayes` package.

In our data setting (8), we use the notation of z_{ij} to denote the j -th element of the z_i vector. Let $\bar{z}_j = \sum_{k=1}^n z_{kj}/n_g$, the j -th component of the sample mean vector $\bar{\mathbf{z}}$. Note that $\sqrt{n}\bar{z}_j \sim N(\sqrt{n}\mu_j^*, 1)$. Therefore, we substitute $\sqrt{n}\bar{z}_i$ for z_i in (12) to eventually obtain the estimate for $\sqrt{n}\mu_j^*$ and divide it by \sqrt{n} .

Subsequently, f -modeling method estimates $(g^*)'(z_i)$ and $g^*(z_i)$ of (11) using the observed data $z_i, i = 1, \dots, n$. This paper uses kernel estimators with normal kernels. See section 2 of [3] for detail. We present the eventual form of the estimator $\hat{\mu}_{EB}$ as follows.

$$(\hat{\boldsymbol{\mu}}_{EB})_i = \widehat{E(\boldsymbol{\mu}_i|\bar{\mathbf{z}})} = \bar{z}_i + \frac{\sum_{j=1}^p (\bar{z}_j - \bar{z}_i) \phi\{\sqrt{n}(\bar{z}_i - \bar{z}_j)/h\}}{h^2 \sum_{j=1}^p \phi\{\sqrt{n}(\bar{z}_i - \bar{z}_j)/h\}}. \quad (13)$$

Here, $(\hat{\boldsymbol{\mu}}_{EB})_i$ denotes the i -th component of $\hat{\boldsymbol{\mu}}_{EB}$, and h the bandwidth of the kernel estimator. Throughout our paper, we use $h = 1/\sqrt{\log p}$, with which good theoretical properties are known to hold (see [3]). It is worth noting that both estimation methods provide the estimator of $\boldsymbol{\mu}^*$ solely from the sample mean $\bar{\mathbf{z}}$.

2.3 Construction of discriminant rules

First, recall that when the prior probability of group 1 and group 2 is provided, the Bayes discriminant rule δ has the form of

$$\delta(\mathbf{x}^{new}) = \left(\mathbf{x}^{new} - \frac{\boldsymbol{\mu}_1 + \boldsymbol{\mu}_2}{2} \right)^\top \boldsymbol{\Sigma}^{-1} (\boldsymbol{\mu}_2 - \boldsymbol{\mu}_1) - \log \frac{p_1}{p_2}, \quad (14)$$

where p_1, p_2 denotes the prior probability of each group. The only difference from (1) is the last term, which denotes the prior odds. In real data situations, when n_1, n_2 samples are obtained from group 1 and group 2, respectively, prior odds can be estimated as n_1/n_2 . As discussed in (3), we can write

$$\delta(\mathbf{x}^{new}) = (\boldsymbol{\mu}_1^* - \boldsymbol{\mu}_2^*)^\top \left(\mathbf{z}^{new} - \frac{\boldsymbol{\mu}_1^* + \boldsymbol{\mu}_2^*}{2} \right) - \log \frac{p_1}{p_2}. \quad (15)$$

As we previously mentioned, we first estimate the precision matrix, decorrelate the data (including \mathbf{x}_{new}), and then estimate the decorrelated mean vector, $\boldsymbol{\mu}^*$. For the classification, we would have two groups of datasets. In each group, we obtain the estimator for the precision matrix $(\hat{\Omega}_1, \hat{\Omega}_2)$. Then, we use the pooled estimator as a final precision estimator. Namely,

$$\hat{\Sigma}^{-1} = \hat{\Omega} = \frac{(n_1 - 1)\hat{\Omega}_1 + (n_2 - 1)\hat{\Omega}_2}{n_1 + n_2 - 2}.$$

For $\mathbf{X}_i \sim N_p(\boldsymbol{\mu}, \Omega^{-1})$, one can write

$$\hat{\Omega}^{1/2} \mathbf{X}_i \sim N_p(\hat{\Omega}^{1/2} \boldsymbol{\mu}, \hat{\Omega}^{1/2} \Omega^{-1} \hat{\Omega}^{1/2}), \quad i = 1, \dots, n.$$

Assuming that $\hat{\Omega}$ estimates Ω properly, $\hat{\Omega}^{1/2} \Omega^{-1} \hat{\Omega}^{1/2}$ can be assumed to be similar to I_p . Therefore, we can apply NPEB and NPMLE methods under desirable settings, to finally get the estimator of $\hat{\Omega}^{1/2} \boldsymbol{\mu}$. Since we have two groups of data, we denote the decorrelated mean of group i and its estimate as $\boldsymbol{\mu}_i^*$ and $\widehat{\boldsymbol{\mu}}_i^*$, respectively ($i = 1, 2$).

Following the procedure, one can obtain the practical version of the discriminant rule as

$$\delta(\mathbf{x}^{new}) = \left(\widehat{\boldsymbol{\mu}}_1^* - \widehat{\boldsymbol{\mu}}_2^* \right)^\top \left(\hat{\Omega}^{1/2} \mathbf{x}^{new} - \frac{\widehat{\boldsymbol{\mu}}_1^* + \widehat{\boldsymbol{\mu}}_2^*}{2} \right) - \log \frac{p_1}{p_2}. \quad (16)$$

Instead of estimating $\boldsymbol{\mu}_1^*$ and $\boldsymbol{\mu}_2^*$ separately, we can estimate $\boldsymbol{\mu}_1^* - \boldsymbol{\mu}_2^*$ at once. When \mathbf{z}_1 and \mathbf{z}_2 denotes the decorrelated sample mean (with true precision matrix) of the group 1 and 2,

$$\mathbf{z}_1 \sim N_p(\boldsymbol{\mu}_1^*, n_1^{-1} I_p), \quad \mathbf{z}_2 \sim N_p(\boldsymbol{\mu}_2^*, n_2^{-1} I_p).$$

Since $\mathbf{z}_1, \mathbf{z}_2$ are independent,

$$\mathbf{z}_1 - \mathbf{z}_2 \sim N_p(\boldsymbol{\mu}_1^* - \boldsymbol{\mu}_2^*, (n_1^{-1} + n_2^{-1}) I_p).$$

Therefore, $\boldsymbol{\mu}_1 - \boldsymbol{\mu}_2$ can be directly estimated from $\mathbf{z}_1 - \mathbf{z}_2$ using NPEB and NPMLE method by multiplying and dividing the constant $a_n = (1/n_1 + 1/n_2)^{-1/2}$. Since the mean difference is considered to be the main key to separate two groups, we can simply plug in $\mathbf{z}_1, \mathbf{z}_2$ for $\boldsymbol{\mu}_1, \boldsymbol{\mu}_2$ in $(\boldsymbol{\mu}_1^* + \boldsymbol{\mu}_2^*)/2$ of (15). Therefore, the classifier built on this method is written as

$$\delta(\mathbf{x}^{new}) = \left(\widehat{\boldsymbol{\mu}_1^* - \boldsymbol{\mu}_2^*}\right)^\top \left(\hat{\Omega}^{1/2} \mathbf{x}^{new} - \frac{\mathbf{z}_1^* + \mathbf{z}_2^*}{2}\right) - \log \frac{p_1}{p_2}. \quad (17)$$

In section 5, we compare (16) and (17)'s performance in real data. We noticed that two discriminant rules show similar performance when same estimation strategies are used. Note that (16) and (17) become identical when one use the estimator of $\boldsymbol{\mu}_1^*$, $\boldsymbol{\mu}_2^*$, and $\boldsymbol{\mu}_1^* - \boldsymbol{\mu}_2^*$ based on sample means. Therefore, we use the discriminant rule (17) for the simulation and theoretical analysis in section 3. We denote 'NPEB1', 'NPMLE1' for the discriminant rule using NPEB, NPMLE method in (17) and 'NPEB2', 'NPMLE2' for (16).

3 Asymptotic results of the NPEB method

In this section, we present the asymptotic result for the discriminant rule with the NPEB method. [18] studied the performance of the discriminant rule (17) when using sample mean. [16] studied the performance of (17) using the mean vector estimator with NPMLE in (11) and showed a region for the parameters related to the strength of mean values and the level of sparsity such that the error rate is asymptotically 0 as the dimension increases. We provide an analogous result for the NPEB method under the setting in [16] and compare the result with those for NPMLE, hard threshold, and naive Bayes rule (which uses the sample mean for (17)).

As in [16] and [18], we assume that the precision matrix is consistently estimated so that the data are decorrelated in an appropriate way, for example, glasso method provides the uniformly consistent estimators of all components in the precision matrix. We emphasize the effects of mean vector estimations after data are decorrelated.

Under (17), assuming $\Sigma = I_p$ or the precision matrix is consistently estimated, the misclassification error rate of a discriminant rule δ is written as

$$\begin{aligned} P\left(\delta(x^{new}) > 0 \mid x^{new} \in \text{group 2}\right) &= P\left((z^{new} - \frac{\bar{z}_1 + \bar{z}_2}{2})^T \hat{\boldsymbol{\mu}}_D^* > 0 \mid z^{new} \sim N_p(\boldsymbol{\mu}_2^*, I)\right) \\ &= \Phi\left\{-\frac{1}{2} \left(\frac{\boldsymbol{\mu}_D^{*T} \hat{\boldsymbol{\mu}}_D^*}{\|\hat{\boldsymbol{\mu}}_D^*\|_2} + \frac{(\bar{z}_1 + \bar{z}_2 - (\boldsymbol{\mu}_1^* + \boldsymbol{\mu}_2^*))^T \hat{\boldsymbol{\mu}}_D^*}{\|\hat{\boldsymbol{\mu}}_D^*\|_2}\right)\right\}, \end{aligned}$$

where $\mu_D^* = \mu_1^* - \mu_2^*$, $\hat{\mu}_D^* = \widehat{\mu_1^* - \mu_2^*}$. Since

$$\bar{z}_1 + \bar{z}_2 - (\mu_1^* + \mu_2^*) \sim N(0, a_n^{-2} I_p),$$

when n_1 and n_2 are fixed, $\bar{z}_1 + \bar{z}_2 - (\mu_1^* + \mu_2^*) = O_p(1)$ holds. Therefore, from the Cauchy-Schwartz inequality, we have

$$\frac{\{\bar{z}_1 + \bar{z}_2 - (\mu_1^* + \mu_2^*)\}^T \hat{\mu}_D^*}{\|\hat{\mu}_D^*\|_2} = O_p(1).$$

Thus, as $p \rightarrow \infty$, we have the result that $P\left(\delta(x^{new}) > 0 \mid x^{new} \in \text{group 2}\right) \rightarrow 0$ is equivalent to

$$V := \frac{\mu_D^{*T} \hat{\mu}_D^*}{\|\hat{\mu}_D^*\|_2} \xrightarrow{P} \infty. \quad (18)$$

This implies that if $V \xrightarrow{P} \infty$ as $p \rightarrow \infty$, a given decision rule δ has the error rate 0 asymptotically. However, as $p/n \rightarrow \infty$, it is widely known that δ has the error rate 1/2 asymptotically, which matches the intuition (see [2]). Therefore, we consider the situation in which both the number of meaningful components (say, the number of ‘signals’) and the degree of signal increase in a positive power of p .

To implement different levels of sparsity of signals in high dimension as $p \rightarrow \infty$, we parametrize the number of nonzero mean differences and their sizes which are commonly used in the study of sparse signals in high dimensional data analysis. See [16] and [5] for the examples. More specifically, we set $\mu_1^* = (0, \dots, 0)$ and $\mu_2^* = (\Delta_l^T, \mathbf{0}_{p-l}^T)$ where Δ_l is the l dimensional column vector with all components Δ . Then we assign

$$\Delta = p^b, l = [p^a] \quad (19)$$

for $b > 0$ and $0 < a < 1$. Δ and l represent the strength of the signal for each component and the level of sparsity, respectively. As p increases, the sparsity level $l = [p^a]$ and the strength of signal Δ are represented as functions of p . This setting was used in the theoretical study by

[16] and the simulation experiments by [5]. This setting will include various forms, including cases where Δ converges to infinity or to zero, in other words, the strength of the signal Δ is very large or very small. This will be accompanied by the number of variables l resulting in comparisons of various methodologies for various cases.

We first set the range of interest for the constants a and b since if either a or b is too large, the two groups can be easily separated regardless of the method used for classification. Therefore, as mentioned in [16], we want to compare various methods only in the (a, b) range as follows:

$$(a, b) \in \mathcal{R} \equiv (T_1 \cup T_2)^c$$

where $T_1 = \{(a, b) \in \mathbb{R}^2, a + 2b \geq 1/2, 0 < a \leq 0.5\}$ and $T_2 = \{(a, b) \in \mathbb{R}^2 : 0.5 < a \leq 1, b > 0\}$. In T_1 or T_2 , the combination of Δ and l provides large strengths of signals leading to clear separation of two groups by various methods. See more details in [16]. We consider the outside of T_1 and T_2 which is $(T_1 \cup T_2)^c$ in comparison of various methods.

Note that if a discriminant rule has the property of (18) in a wider range of (a, b) than another one, then the first discriminant rule has superiority to the other one asymptotically. [16] derived some conditions on (a, b) under which the classifier (17) using the NPMLE, the sample mean, and hard threshold method achieves (18). [16] showed that the discriminant rule with NPMLE has an advantage over naive Bayes rule and hard threshold in that (18) of NPMLE method is obtained in a wider range than the other two methods.

Here, we suggest the range of parameters to achieve (18) in the NPEB method and compare this with the regions of NPMLE, the sample mean(SM), and hard threshold(Hard) methodologies in the following theorem. We first define $\mathcal{R}_{NPEB}, \mathcal{R}_{NPMLE}, \mathcal{R}_{SM}$ and \mathcal{R}_{Hard} as the areas of (a, b) satisfying (18) under the corresponding mean estimation methods.

Theorem 1. *Suppose $\mu_1 = (0, \dots, 0)$ and $\mu_2 = (\Delta_l^T, \mathbf{0}_{p-l}^T)$ where $\Delta = p^b, l = [p^a]$. Then, $\mathcal{R}_{NPEB}, \mathcal{R}_{NPMLE}$ cover both \mathcal{R}_{SM} and \mathcal{R}_{Hard} . Specifically,*

$$\mathcal{R}_{Hard} = C, \mathcal{R}_{SM} = D,$$

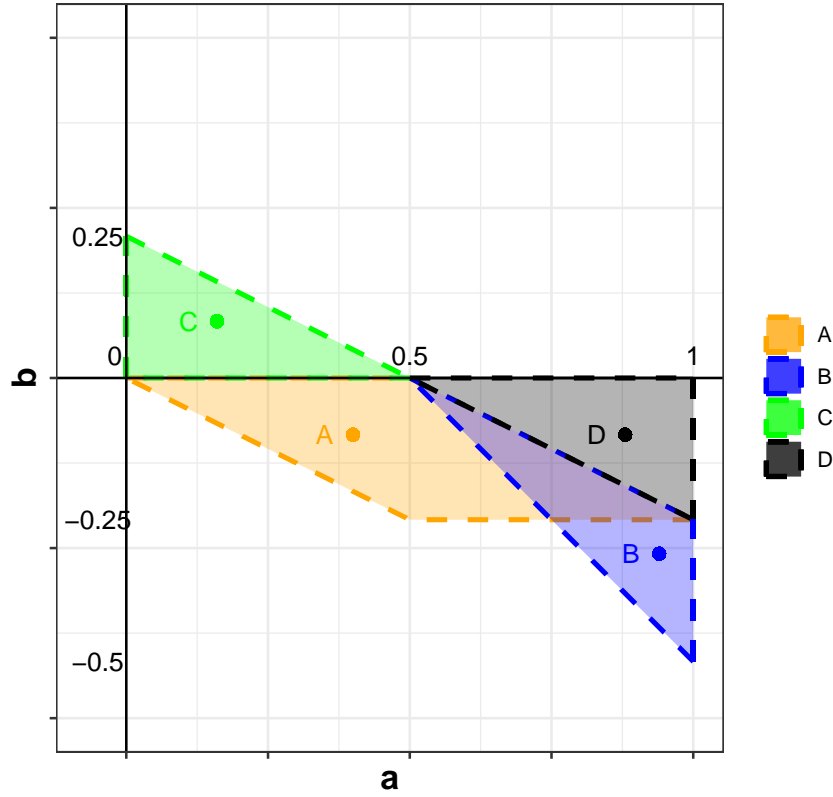


Figure 1: The area of (a, b) under the setting (19)

$$\mathcal{R}_{NPEB} \supset A \cup C \cup D, \mathcal{R}_{NPMLE} \supset B \cup C \cup D,$$

where

$$A = \{(a, b) \in \mathbb{R}^2, 0 \leq a + 2b \leq 1/2 : -0.25 < b < 0 \text{ and } 0 < a < 1\},$$

$$B = \{(a, b) \in \mathbb{R}^2, a + b \geq 1/2 : -0.5 < b < 0 \text{ and } 0.5 < a < 1\},$$

$$C = \{(a, b) \in \mathbb{R}^2, a + 2b \leq 1/2 : 0 < b < 0.25 \text{ and } 0 < a < 0.5\},$$

$$D = \{(a, b) \in \mathbb{R}^2, a + 2b \geq 1/2 : -0.25 < b < 0 \text{ and } 0.5 < a < 1\}.$$

Proof. See Appendix. □

Note that \mathcal{R}_{NPEB} and \mathcal{R}_{NPMLE} can be enlarged further, while \mathcal{R}_{SM} and \mathcal{R}_{Hard} exactly matches with D and C . The visual illustration of each region is in figure 1. We can see that the NPEB method covers all the areas of the naive Bayes rule and hard threshold method. On the other hand, neither \mathcal{R}_{NPEB} nor \mathcal{R}_{NPMLE} is included in each other. Both methods are expected to work well in both sparse and dense cases while the hard threshold method and naive Bayes rule are designed for only sparse and dense cases, respectively.

We provide numerical studies in section 4 and real data analysis in 5 to compare these methods, and see that there doesn't seem to be any tendency that either of NPMLE and NPEB dominates the other method.

4 Simulations

In this section, we provide simulation results for various combinations of mean vectors and covariance matrices. We divided simulation settings according to the sparseness and denseness of the precision matrix and those of the difference of mean vectors.

Under the assumption of multivariate normal distribution, $\Omega_{ij} = 0$ means that X_i and X_j are conditionally independent. To verify the strength of glasso and LAM methods separately, we divided simulation settings according to the sparseness of the precision matrix or covariance matrix. To compare the mean vector estimation method individually, we assumed the simulation setting as follows. We set $\mu_1^T = (0, \dots, 0)$, $\mu_2^T = (\Delta_l^T, 0_{p-l}^T)$ where Δ_l is the l dimensional column vector with all component Δ and $\mathbf{0}_{p-l}$ is the $(p-l)$ dimensional vector with all 0 components. In some situation, we set $\mu_{2s} = \Sigma^{1/2}\mu_2 = (\Delta_l^T, \mathbf{0}_{p-l}^T)$. Throughout the simulation, we set $p = 500$ with the number of training data and test data as $n_{1,train} = n_{2,train} = 50$ and $n_{1,test} = n_{2,test} = 250$.

We consider the following simulation settings for various configurations of l and Δ as well as different structure of Σ .

1. Setting 1: AR(1) structured precision matrix. We set Σ^{-1} as $(\Sigma^{-1})_{ij} = \rho^{|i-j|}$.

-simulation 1-1: $\Delta = 3, l = 20$ in μ_{2s} with $\rho = 0.8$.

- simulation 1-2: $\Delta = 0.4, l = 400$ in μ_{2s} with $\rho = 0.8$.
2. Setting 2: Blocked AR(1) structured precision matrix. We set Σ^{-1} as
$$\begin{bmatrix} \Sigma_q^{-1} & 0 \\ 0 & I_{p-q} \end{bmatrix},$$
 where $(\Sigma_q^{-1})_{ij} = \rho^{|i-j|}$ for $1 \leq i, j \leq q$.
- simulation 2-1: $\Delta = 3, l = 20$ in μ_{2s} with $\rho = 0.9, q = 50$.
- simulation 2-2: $\Delta = 0.15, l = 400$ in μ_{2s} with $\rho = 0.9, q = 50$.
3. Setting 3: Exchangeable precision matrix. We set Σ^{-1} as $(\Sigma^{-1})_{ij}$ to have 1 as a diagonal components and ρ as all off-diagonal elements.
- simulation 3-1: $\Delta = 0.7, l = 20$ in μ_2 with $\rho = 0.3$.
- simulation 3-2: $\Delta = 0.07, l = 20$ in μ_{2s} with $\rho = 0.3$.
4. Setting 4: Toeplitz covariance matrix. We set Σ as $\Sigma_{ij} = 1 / (|i - j| + 1)$.
- simulation 4-1: $\Delta = 1, l = 20$ in μ_2 .
- simulation 4-2: $\Delta = 0.4, l = 20$ in μ_{2s} .
5. Setting 5: Banded covariance matrix. We set Σ as $\Sigma_{ij} = \max(1 - |i - j| / 10, 0)$.
- simulation 5-1: $\Delta = 0.7, l = 20$ in μ_2 .
- simulation 5-2: $\Delta = 0.6, l = 20$ in μ_{2s} .

We present misclassification error rates in Table 1 to Table 5, in which the columns and rows denote the precision matrix and mean vector estimation methods, respectively. We also provide the error rates obtained when the true precision matrix is used instead of estimators, denoted as ‘Oracle.prec’, to verify the effect of the precision matrix estimation. Additionally, we analyze the error rate with a precision matrix estimator which is diagonal and each entry is an inverse of the sample variance of each feature, denoted as ‘IR’. We summarize the result as follows :

- *Impact of decorrelation of the LAM on the mean vector estimations:*

From all the results from the LAM and the IR, we noticed that mean vector estimation

methods have a consistent impact on the error rates. Especially the SM method is improved by the NPMLE, and the NPEB since the error rates of the NPEB and the NPMLE methods are smaller than those of the SM.

- *Impact of decorrelation using glasso on the mean vector estimations:*

When the precision matrix is estimated by glasso, the mean vector estimation itself didn't show a clear impact on the error rate. NPEB and NPMLE methods with the decorrelation using glasso method do not significantly improve the error rate of SM & glasso based discriminant rule.

- *Impact of glasso and LAM:*

Depending on the structure of the covariance matrix or precision matrix, the glasso and the LAM are designed for sparse and general structures, respectively. For example, in simulation 2-1, the glasso method tends to produce smaller error rates than those from the LAM method. Simulation 2-1 shows the sparse structure of the precision matrix since the AR(1) structure is the banded matrix. On the other hand, in situation 3-1, using the precision matrix with all the same off-diagonal terms, the LAM method performs better than glasso method since the precision matrix in simulation 3-1 is a dense matrix. These two simulations coincide with the effect of the glasso and the LAM on the different structures of the precision matrix, such as sparsity and denseness.

- *No uniform dominance among precision estimation strategies:*

Comparing the results in simulations 2-1 and 2-2, one can notice that even though two situations are generated with the same precision matrix, a tendency in error rates is dissimilar. In situation 2-1, the linear discriminant rule using the graphical lasso method shows the lowest error rate with every mean estimation strategy, which is completely opposite to simulation 2-2. Therefore, the dominant precision estimation strategy for the linear discriminant rule cannot be determined depending on the precision matrix only.

- *Comparison with theoretical result:*

The theoretical result can elucidate the significant dominance of the NPMLE and NPEB method over the SM method in simulations 1-2 and 2-2 under the IR and LAM method for the estimation of the precision matrix. According to theorem 1, when there is a dense signal with low signal intensity ($5/6 < a < 1$, $b < 0$), the NPMLE and NPEB methods ensure a wider range of b in which the asymptotic error rate is zero compared to SM method. One can check that simulation 1-2 and 2-2 nearly falls into this area.

- *Impact of mean vector estimation by shrinkage:*

From the results in simulations 3-1 and 3-2, we can observe conspicuous improvements in the SM method in error rates by using the NPMLE and NPEB methods for any given estimation of the precision matrix. When the sparse signals have an intensity that is proportional to the positive power of p , namely, when $0 < a < 1/2$, $0 < b < 1/4$, and $a + 2b < 1/2$ holds, the linear discriminant rules built from the SM method are known to asymptotically act as random guessing, while the discriminant rules using NPEB and NPMLE have the error rate which asymptotically converges to zero.

5 Real Data Analysis

In this section, we consider five real data sets to compare the performance of various binary classification methods discussed in this paper. Through these real data examples, we investigate the role of mean vector and precision matrix estimation in high-dimensional classification.

Four real datasets are used for comparing the performance of discriminant rules.

- EEG data: 122 observations (77: group 1, 45: group 2) with 512 features

We used EEG (Electroencephalography) data to validate linear discriminant rules under multiple estimation methods (which is available at <https://archive.ics.uci.edu/ml/datasets/eeg+database>). The data was initially generated for the large study about the genetic predisposition of alcoholism. Measurements from 64 electrodes placed on the subject's scalps were sampled at 256 Hz for 1 second. For data

	Simulation 1-1				Simulation 1-2			
	Oracle.prec	glasso	LAM	IR	Oracle.prec	glasso	LAM	IR
NPEB1	0.0000 (0.0000)	0.1374 (0.0156)	0.0468 (0.0093)	0.0644 (0.0113)	0.0001 (0.0004)	0.4079 (0.0215)	0.3236 (0.0200)	0.3053 (0.0201)
NPEB2	0.0000 (0.0000)	0.1375 (0.0158)	0.1139 (0.0144)	0.1146 (0.0146)	0.0001 (0.0004)	0.4084 (0.0219)	0.3099 (0.0206)	0.2840 (0.0196)
NPMLE1	0.0000 (0.0000)	0.1370 (0.0157)	0.0324 (0.0078)	0.0520 (0.0101)	0.0000 (0.0000)	0.4073 (0.0217)	0.2288 (0.0183)	0.1422 (0.0162)
NPMLE2	0.0000 (0.0000)	0.1375 (0.0156)	0.0939 (0.0130)	0.0988 (0.0138)	0.0000 (0.0000)	0.4079 (0.0218)	0.1379 (0.0148)	0.0489 (0.0099)
SM	0.0000 (0.0000)	0.1393 (0.0157)	0.1945 (0.0178)	0.1854 (0.0177)	0.0003 (0.0007)	0.4081 (0.0220)	0.4352 (0.0213)	0.4344 (0.0212)

Table 1: Simulation 1 result

	Simulation 2-1				Simulation 2-2			
	Oracle.prec	glasso	LAM	IR	Oracle.prec	glasso	LAM	IR
NPEB1	0.0000 (0.0000)	0.0690 (0.0115)	0.1235 (0.0147)	0.1692 (0.0172)	0.0952 (0.0132)	0.3184 (0.0211)	0.1997 (0.0179)	0.1205 (0.0136)
NPEB2	0.0000 (0.0000)	0.0686 (0.0115)	0.1522 (0.0156)	0.1692 (0.0169)	0.0946 (0.0128)	0.3191 (0.0206)	0.1708 (0.0162)	0.1168 (0.0139)
NPMLE1	0.0000 (0.0000)	0.0687 (0.0116)	0.1199 (0.0148)	0.1609 (0.0164)	0.0868 (0.0126)	0.3196 (0.0211)	0.2036 (0.0167)	0.1112 (0.0139)
NPMLE2	0.0000 (0.0000)	0.0688 (0.0115)	0.1534 (0.0164)	0.1665 (0.0167)	0.0883 (0.0131)	0.3192 (0.0211)	0.2197 (0.0189)	0.1032 (0.0135)
SM	0.0000 (0.0000)	0.0708 (0.0116)	0.1665 (0.0157)	0.2682 (0.0198)	0.2002 (0.0181)	0.3208 (0.0208)	0.2957 (0.0203)	0.2253 (0.0190)

Table 2: Simulation 2 result

	Simulation 3-1				Simulation 3-2			
	Oracle.prec	glasso	LAM	IR	Oracle.prec	glasso	LAM	IR
NPEB1	0.0000 (0.0000)	0.2609 (0.0194)	0.1285 (0.0145)	0.1291 (0.0144)	0.0720 (0.0112)	0.2042 (0.0170)	0.0830 (0.0120)	0.0834 (0.0122)
NPEB2	0.0000 (0.0000)	0.2629 (0.0198)	0.1874 (0.0174)	0.1887 (0.0172)	0.0992 (0.0130)	0.2048 (0.0173)	0.1140 (0.0139)	0.1179 (0.0143)
NPMLE1	0.0000 (0.0000)	0.2611 (0.0196)	0.1130 (0.0137)	0.1154 (0.0142)	0.0648 (0.0110)	0.2047 (0.0168)	0.0724 (0.0113)	0.0728 (0.0114)
NPMLE2	0.0000 (0.0000)	0.2625 (0.0199)	0.1705 (0.0169)	0.1784 (0.0167)	0.0897 (0.0126)	0.2041 (0.0173)	0.1019 (0.0129)	0.1094 (0.0141)
SM	0.0000 (0.0000)	0.2656 (0.0200)	0.2550 (0.0194)	0.2503 (0.0190)	0.1861 (0.0171)	0.2088 (0.0172)	0.1977 (0.0173)	0.1936 (0.0173)

Table 3: Simulation 3 result

	Simulation 4-1				Simulation 4-2			
	Oracle.prec	glasso	LAM	IR	Oracle.prec	glasso	LAM	IR
NPEB1	0.1888 (0.0172)	0.1990 (0.0178)	0.1554 (0.0155)	0.1625 (0.0159)	0.2601 (0.0198)	0.2523 (0.0190)	0.2024 (0.0171)	0.2107 (0.0176)
NPEB2	0.2424 (0.0185)	0.1985 (0.0177)	0.1612 (0.0164)	0.1684 (0.0168)	0.3314 (0.0212)	0.2527 (0.0192)	0.2150 (0.0180)	0.2191 (0.0184)
NPMLE1	0.1691 (0.0159)	0.1983 (0.0178)	0.1536 (0.0155)	0.1610 (0.0162)	0.2385 (0.0187)	0.2524 (0.0191)	0.2020 (0.0175)	0.1610 (0.0162)
NPMLE2	0.2241 (0.0182)	0.1985 (0.0176)	0.1579 (0.0161)	0.1666 (0.0167)	0.3215 (0.0217)	0.2530 (0.0192)	0.2127 (0.0185)	0.1666 (0.0167)
SM	0.2998 (0.0208)	0.2015 (0.0180)	0.1944 (0.0172)	0.1919 (0.0169)	0.3660 (0.0217)	0.2558 (0.0192)	0.2448 (0.0187)	0.2422 (0.0190)

Table 4: Simulation 4 result

	Simulation 5-1				Simulation 5-2			
	Oracle.prec	glasso	LAM	IR	Oracle.prec	glasso	LAM	IR
NPEB1	0.0960 (0.0134)	0.3562 (0.0209)	0.3077 (0.0203)	0.3055 (0.0215)	0.1164 (0.0144)	0.1346 (0.0147)	0.1060 (0.0133)	0.1004 (0.0131)
NPEB2	0.1250 (0.0146)	0.3592 (0.0207)	0.3224 (0.0211)	0.3190 (0.0212)	0.1732 (0.0165)	0.1363 (0.0149)	0.1124 (0.0134)	0.1026 (0.0135)
NPMLE1	0.0926 (0.0130)	0.3559 (0.0212)	0.3059 (0.0203)	0.3005 (0.0210)	0.1040 (0.0131)	0.1341 (0.0147)	0.1045 (0.0133)	0.0992 (0.0130)
NPMLE2	0.1131 (0.0143)	0.3579 (0.0207)	0.3206 (0.0209)	0.3135 (0.0207)	0.1611 (0.0159)	0.1358 (0.0150)	0.1112 (0.0134)	0.1019 (0.0133)
SM	0.2020 (0.0174)	0.3633 (0.0212)	0.3667 (0.0207)	0.3464 (0.0216)	0.2451 (0.0194)	0.1397 (0.0152)	0.1377 (0.0151)	0.1166 (0.0139)

Table 5: Simulation 5 result

pre-processing, we parsed this time series data into 8 intervals and extracted each interval's median value. Therefore, we finally made the data of $64 \times 8 = 512$ dimensional vectors from each subject. With 122 observations in sum ($n_1 = 77$ subjects from the alcoholic group and $n_2 = 45$ from the control group), we examined the performance of each discriminant rule using the LOOCV method.

- Gravier data: 168 observations (111: group 1, 57: group 2) with 1000 features

Gene array data obtained for the study pertaining to the prediction of metastasis of small node-negative breast carcinoma is also utilized, which we named Gravier data. Small invasive ductal carcinomas without axillary lymph node involvement (T1T2N0) were analyzed from 168 patients. Among these, 111 subjects who had no events for 5 years afterward were categorized as group 1, and the other 57 subjects with early metastasis were assigned as group 2. We processed the original data by extracting 1000 features that have the most significant t values among the 2905 features beforehand.

- Ham data: 214 observations (111: group 1, 103: group 2) with 431 features.

Ham data was obtained by food spectrograph about 19 Spanish and 18 French dry-cured hams. A food spectrograph is utilized in chemometrics to classify food types, which can be directly used to assure food safety and quality. This data is publicly available at <http://www.timeseriesclassification.com/description.php?Dataset=Ham>. From 37 hams in total, up to 6 observations were obtained. Therefore, 214 observations were categorized into two groups (111 observations for group 1 and 103 for group 2), with 431 feature vectors for each observation. The data preprocessing procedure is described in 'Sodium dodecyl sulphate-polyacrylamide gel electrophoresis of proteins in dry-cured hams: Data registration and multivariate analysis across multiple gels' (to be in reference).

- IMVigor data: 298 observations (230: group 1, 68: group 2) with 4792 features (divided into 7 groups)

Clinical outcomes of metastatic urothelial cancer patients were collected and are available at <http://research-pub.gene.com/IMvigor210CoreBiologies/> (see [15]). Observations about 230 non-responders and 68 responders are composed of 4792 feature vectors. These features are known to be correlated within seven groups, which contain 1583, 975, 569, 548, 546, 341, and 230 features each. Therefore, we investigated the error rate of linear discriminant rules with and without this group information.

Within these data, classification performance has been measured through Leave-One-Out Cross Validation (LOOCV) method. As introduced in 2.3, linear discriminant rules can be constructed by estimating μ_1^* and μ_2^* respectively, or $\mu_2^* - \mu_1^*$ at once. Therefore, we compared the error rate of each discriminant rule according to the mean estimation method, precision estimation method, and discriminant rule construction method.

As one can see from Table 6, classification errors largely depend on precision matrix estimation methods. A more suitable precision estimation method relies on the data. For example, in HAM data, the LAM method shows a lower error rate, while glasso method performs well with Gravier data. Among mean vector estimation methods, error rates do not vary significantly. However, when classifying Gravier data with glasso precision estimation method, the error rate varied significantly according to the mean estimation method. Therefore, we compared each component of $\widehat{\mu_2^* - \mu_1^*}$ among mean estimation methods.

Figure 2 shows the plots of NPEB vs. SM and NPMLE vs. SM after two methods of decorrelation. The NPEB and NPMLE tend to have the shrinkage effect of the SM, especially for large SM values. It is seen that the NPMLE in (11) with the estimated \hat{G} has the monotonicity property of SM. On the other hand, the NPEB with estimated marginal density \hat{f} and \hat{f}' is not guaranteed to have monotonicity, so there exist some wiggly patterns in local regions, however, overall patterns of NPEB are similar to those of NPMLE. In general, the posterior mean in (11) based on f -modeling is not guaranteed to have the monotonicity in z while the g -modeling such as plugging in estimated \hat{G} into (11) guarantees the monotonicity in z . See the discussion on this issue in [11] for the Poisson model, which is also true for the case of normal mean estimation.

	EEG			Gravier			Ham			IMVigor		
	glasso	LAM	IR	glasso	LAM	IR	glasso	LAM	IR	glasso	LAM	IR
NPEB1	*22/122	24/122	27/122	*19/168	32/168	24/168	39/214	31/214	49/214	169/298	71/298	111/298
NPEB2	23/122	28/122	28/122	31/168	33/168	31/168	33/214	*30/214	53/214	104/298	*70/298	111/298
NPMLE1	23/122	26/122	27/122	26/168	31/168	29/168	40/214	32/214	49/214	128/298	*70/298	112/298
NPMLE2	24/122	26/122	27/122	30/168	33/168	31/168	33/214	*30/214	52/214	106/298	*70/298	110/298
SM	24/122	26/122	28/122	31/168	33/168	31/168	34/214	*30/214	50/214	106/298	*70/298	111/298

Table 6: LOOCV classification result about EEG, Gravier, Ham, and IMVigor datasets of corresponding discriminant rules. ‘*’ indicates the lowest error rate in each data set.

To summarize, the correlation, such as glasso and LAM methods, is effective in most of the cases in that the IR without decorrelation is improved although those two methods make the IR worse in some data sets. In particular, the glasso is sensitive to different cases since the glasso is designed for a sparse structured precision matrix. On the other hand, the LAM method is robust to all data sets except Gravier data in which the performance of all classification methods is worse than the glasso and the IR. For the glasso method, different classification methods have large variations in error rate while the LAM method produces quite similar error rates for different rules.

6 Concluding Remarks

Combining different types of precision matrix and mean vector estimation strategies, we investigate the performances of the various linear discriminant rules. We evaluate these rules under various contrived settings. With dense and sparse structures of precision matrices and the difference of mean vectors, the performances of the discriminant rules are investigated. We, therefore, observe that linear discriminant rules perform well when the simulation situation is aligned with the assumptions that each estimation strategy is based on. Our results including numerical studies and real data examples show that none of the discriminant rules tend to dominate the others. In particular, we emphasize that the theoretical result is presented on the NPEB. We believe that this is an interesting result in the sense that we can compare f -modeling and g -modeling theoretically, which are corresponding to the NPEB and NPMLE where the performance of the NPMLE is studied in [16].

One interesting phenomenon is that the structure of the mean vector may be changed after

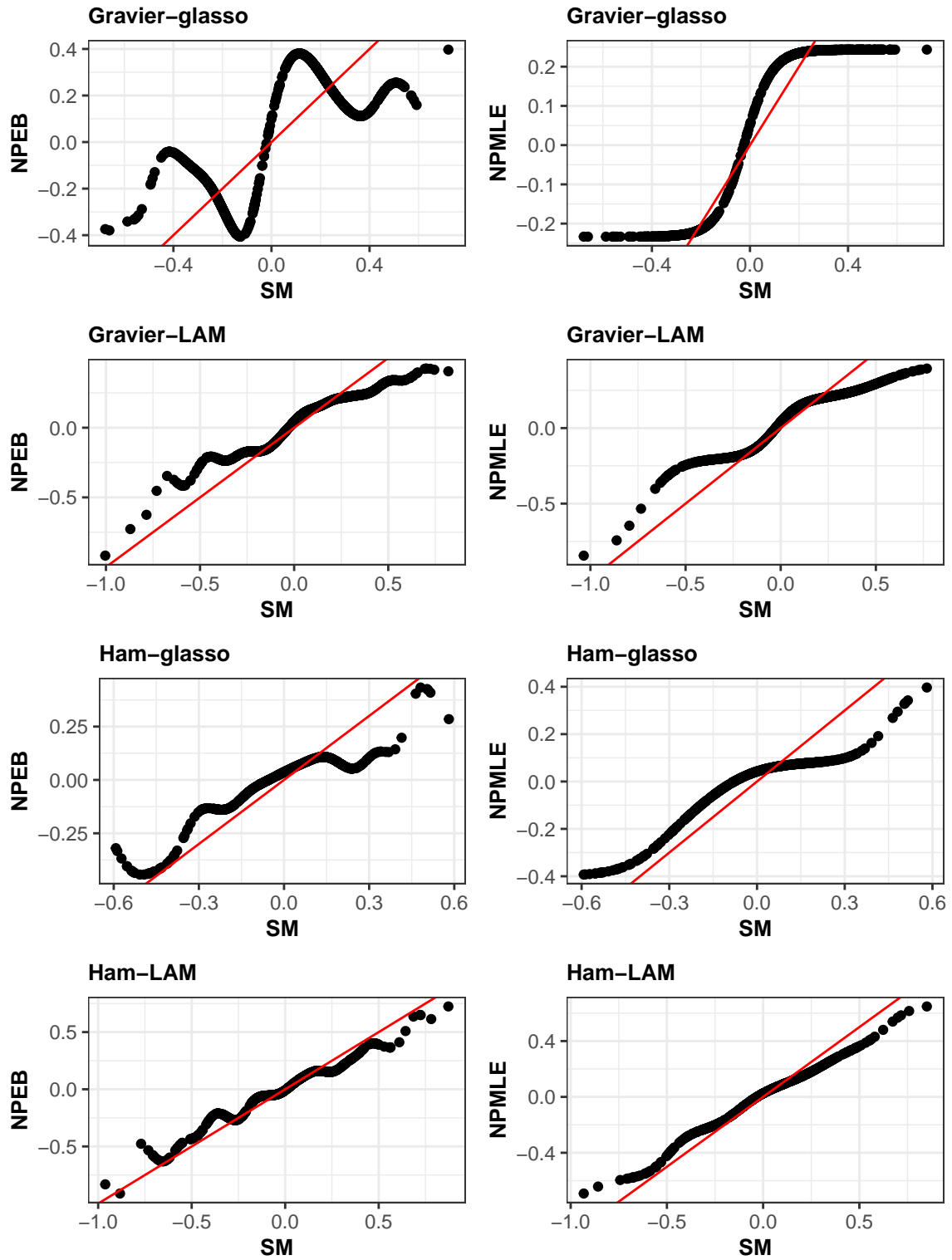


Figure 2: $(\widehat{\mu}_2^* - \widehat{\mu}_1^*)$ plot - NPEB, NPMLE method to SM method

decorrelation. Since our results in this paper show that the different methods of estimation of mean vectors have different performances depending on the structure of mean vectors, so it will be interesting to investigate the changes in mean vector structures after decorrelation and their effect on the choice of estimation methods. We leave this as future work.

Acknowledgement

Research of J. Park was supported by the National Research Foundation of Korea (NRF) grant funded by the Korea government (MSIT) (No. 2020R1A2C1A01100526).

References

- [1] ANDERSON, T. An Introduction to Multivariate Statistical Analysis. Wiley Series in Probability and Statistics. Wiley, 2003.
- [2] BICKEL, P. J., AND LEVINA, E. Some theory for fisher's linear discriminant function, naive bayes', and some alternatives when there are many more variables than observations. Bernoulli 10, 6 (2004), 989–1010.
- [3] BROWN, L. D., AND GREENSHTEIN, E. Nonparametric empirical bayes and compound decision approaches to estimation of a high-dimensional vector of normal means. The Annals of Statistics (2009), 1685–1704.
- [4] CAI, T., LIU, W., AND LUO, X. A constrained l_1 minimization approach to sparse precision matrix estimation. Journal of the American Statistical Association 106, 494 (2011), 594–607.
- [5] DICKER, L. H., AND ZHAO, S. D. High-dimensional classification via nonparametric empirical Bayes and maximum likelihood inference. Biometrika 103, 1 (02 2016), 21–34.
- [6] EFRON, B. Empirical bayes estimates for large-scale prediction problems. Journal of the American Statistical Association 29, 487 (2009), 1015–1028.

- [7] EFRON, B. Two modeling strategies for empirical bayes estimation. Statistical science: a review journal of the Institute of Mathematical Statistics 29, 2 (2014), 285.
- [8] FAN, J., AND FAN, Y. High dimensional classification using features annealed independence rules. The Annals of statistics 36, 6 (2008), 2605.
- [9] FRIEDMAN, J., HASTIE, T., AND TIBSHIRANI, R. Sparse inverse covariance estimation with the graphical lasso. Biostatistics 9, 3 (2008), 432–441.
- [10] GREENSHTEIN, E., AND PARK, J. Application of non parametric empirical bayes estimation to high dimensional classification. Journal of Machine Learning Research 10, 7 (2009).
- [11] IGNATIADIS, N., AND WAGER, S. Confidence intervals for nonparametric empirical bayes analysis. Journal of the American Statistical Association (2022), 1–18.
- [12] JIANG, W., AND ZHANG, C.-H. General maximum likelihood empirical bayes estimation of normal means. The Annals of Statistics 37, 4 (2009), 1647–1684.
- [13] KOENKER, R., AND MIZERA, I. Convex optimization in r. Journal of Statistical Software 60 (2014), 1–23.
- [14] LAM, C. Nonparametric eigenvalue-regularized precision or covariance matrix estimator. The Annals of Statistics 44, 3 (2016), 928–953.
- [15] MARIATHASAN, S., TURLEY, S. J., NICKLES, D., CASTIGLIONI, A., YUEN, K., WANG, Y., KADEL III, E. E., KOEPPEN, H., ASTARITA, J. L., CUBAS, R., ET AL. Tgf β attenuates tumour response to pd-l1 blockade by contributing to exclusion of t cells. Nature 554, 7693 (2018), 544–548.
- [16] PARK, H., BAEK, S., AND PARK, J. High-dimensional linear discriminant analysis using nonparametric methods. Journal of Multivariate Analysis 188 (2022), 104836.

- [17] SAHA, S., AND GUNTUBOYINA, A. On the nonparametric maximum likelihood estimator for gaussian location mixture densities with application to gaussian denoising. The Annals of Statistics 48, 2 (2020), 738–762.
- [18] WANG, C., AND JIANG, B. On the dimension effect of regularized linear discriminant analysis. Electronic Journal of Statistics 12 (2018), 2709–2742.

A Lemmas for Theorem 1

We present the following four lemmas which are used in the proof of Theorem 1.

Lemma 1. For $p > 1$,

$$\left(1 - \frac{1}{p^2}\right)^p \geq 1 - \frac{1}{p}. \quad (20)$$

Proof. One can easily show that $f(x) = x \log\left(\frac{x+1}{x}\right)$ is an increasing function, by checking

$$f'(x) = \log\left(\frac{x+1}{x}\right) - \frac{1}{x+1}, \quad f''(x) = -\frac{1}{x(x+1)^2} < 0$$

and $\lim_{x \rightarrow \infty} f'(x) = 0$. From $f(p) \geq f(p-1)$, one can obtain

$$p \log\left(1 - \frac{1}{p^2}\right) \geq \log\left(1 - \frac{1}{p}\right),$$

which concludes the proof. □

Lemma 2. Let $Z_1, \dots, Z_p \stackrel{\text{iid}}{\sim} N(0, 1)$ and $\Delta = p^b$. For $b < 0$ and the fixed constant $a_n = (1/n_1 + 1/n_2)^{-1/2}$,

$$P\left(\max_{1 \leq j \leq p} |Z_j| + a_n \Delta < \log p\right) > 1 - \frac{1}{p} \quad (21)$$

holds for large enough p .

Proof. Noting that for all $t > 0$, we have

$$\frac{t}{t^2 + 1} \phi(t) < 1 - \Phi(t) \leq \frac{1}{t} \phi(t)$$

where ϕ, Φ denote the probability distribution function and the cumulative distribution function of standard normal distribution. Then we obtain

$$P \left(\max_{1 \leq j \leq p} |Z_j| + a_n \Delta < \log p \right) = \{1 - 2\Phi(a_n \Delta - \log p)\}^p \geq \left\{ 1 - \frac{2\phi(\log p - a_n \Delta)}{\log p - a_n \Delta} \right\}^p. \quad (22)$$

Since $a_n \Delta \rightarrow 0$ and $\log p \rightarrow \infty$ as $p \rightarrow \infty$, we have $2a_n \Delta < \log p$ for large p , therefore (22) satisfies the followings:

$$\begin{aligned} \left\{ 1 - \frac{2\phi(\log p - a_n \Delta)}{\log p - a_n \Delta} \right\}^p &\geq \left[1 - \frac{4\phi\{(\log p)/2\}}{\log p} \right]^p \\ &= \left[1 - \frac{4}{\sqrt{2\pi} \log p} \exp\{-(\log p)^2/8\} \right]^p. \end{aligned}$$

From lemma 1, for large p satisfying

$$\frac{4}{\sqrt{2\pi} \log p} \exp\left\{-\frac{(\log p)^2}{8}\right\} \leq \frac{1}{p^2},$$

we obtain

$$P \left(\max_{1 \leq j \leq p} |Z_j| + a_n \Delta < \log p \right) \geq \left(1 - \frac{1}{p^2} \right)^p \geq 1 - \frac{1}{p}.$$

□

Lemma 3. Let $Z_i \sim N(0, 1)$ and $\Delta = p^b$. Then, for $b < 0$ and $a_n = (1/n_1 + 1/n_2)^{-1/2}$, we

have

$$P\left(|Z_i| + a_n\Delta < \sqrt{2\alpha(\log p + 1)}\right) > 1 - \frac{8}{\sqrt{2\alpha \log p}} \frac{e}{\sqrt{2\pi}p^\alpha} \quad (23)$$

for large enough p .

Proof. From the fact

$$\frac{t}{t^2 + 1}\phi(t) < 1 - \Phi(t) \leq \frac{1}{t}\phi(t),$$

for large enough p which satisfy $a_n\sqrt{2\alpha(\log p + 1)} < p^{-b} = 1/\Delta$ and $\sqrt{2\alpha(\log p + 1)} - 1 > \sqrt{2\alpha \log p}/2$, we obtain

$$\begin{aligned} & P\left(|Z_i| + a_n\Delta < \sqrt{2\alpha(\log p + 1)}\right) \\ &= 1 - 2\Phi\left(\sqrt{2\alpha(\log p + 1)} - a_n\Delta\right) \\ &> 1 - \frac{2}{\sqrt{2\pi}} \frac{2}{\sqrt{2\alpha(\log p + 1)} - a_n\Delta} \exp\left\{-\frac{1}{2}(\sqrt{2\alpha(\log p + 1)} - a_n\Delta)^2\right\} \\ &> 1 - \frac{4}{\sqrt{2\alpha(\log p + 1)} - 1} \frac{1}{\sqrt{2\pi}p^\alpha} \exp\left\{a_n\Delta\sqrt{2\alpha(\log p + 1)}\right\} \\ &> 1 - \frac{8}{\sqrt{2\alpha \log p}} \frac{e}{\sqrt{2\pi}p^\alpha}. \end{aligned}$$

□

Lemma 4. For $\widehat{\mu}_{D,i}^{EB}$ defined in (31), we have the lower bound W_i such that

$$\sum_{i=1}^{p_1} \widehat{\mu}_{D,i}^{EB} \geq \sum_{i=1}^{p_1} W_i \geq \frac{h^2}{1+h^2} a_n p^{a+b} \{1 + o(1)\} + o_p\{(\log p)^2\}$$

where

$$W_i = \begin{cases} W_{1i}, & \text{if } |Z_i| + a_n\Delta \leq \sqrt{2\alpha(\log p + 1)} \\ W_{2i}, & \text{o.w} \end{cases}, \quad (24)$$

and

$$W_{1i} = \frac{h^2 Z_i^*}{1+h^2} - \frac{h^2}{1+h^2} \frac{(1+2\sqrt{2\pi}p^{1/2+\epsilon})\sqrt{2\alpha(\log p+1)} + (1+h^2)/h^4}{p^{1-\alpha}(1-p^{a-1}) - 2p^{1/2+\epsilon}},$$

$$W_{2i} = \Delta + \frac{1}{a_n}(1-\log p)Z_i - \frac{1}{a_n h^2} \log p.$$

Here, $Z_i^* = Z_i + a_n \Delta$.

Proof. As this proof contains several technical details, we first summarize the flow of the proof. We obtain the first inequality by introducing the auxiliary random variable V_i which satisfies $\widehat{\mu}_{D,i}^{EB} \geq V_i \geq W_i$. Note that the random variable W_i is independent. The second inequality is shown by using the weak law of large numbers (WLLN).

- First, we consider an auxiliary random variable V_i as the following one :

$$V_i = \begin{cases} V_{1i}, & \text{if } |Z_i| + a_n \Delta \leq \sqrt{2\alpha(\log p + 1)} \\ V_{2i}, & \text{o.w} \end{cases} \quad (25)$$

where

$$V_{1i} = \Delta + \frac{Z_i}{a_n} - \frac{1}{h^2} \frac{\frac{1}{\sqrt{2\pi}} \frac{h^3}{(1+h^2)^{3/2}} \{(p_1-1)Z_i T_i + (p-p_1)Z_i^* T_i^*\} + 2p^{1/2+\epsilon}}{\frac{1}{\sqrt{2\pi}} + \frac{1}{\sqrt{2\pi}} \frac{h}{(1+h^2)^{1/2}} \{(p_1-1)T_i + (p-p_1)T_i^*\} - 2p^{1/2+\epsilon}},$$

$$V_{2i} = \Delta + \frac{Z_i}{a_n} + \frac{1}{a_n h^2} \min \{(Z_{ji}^-)_{1 \leq j \leq p_1}, (Z_{ji}^- + a_n \Delta)_{p_1+1 \leq j \leq p}\}.$$

Here, Z_{ij}^- , Z_i^* , T_i , T_i^* are defined as follows.

$$Z_{ij}^- = Z_i - Z_j, \quad Z_i^* = Z_i + a_n \Delta,$$

$$T_i = \exp \left\{ -\frac{Z_i^2}{2(1+h^2)} \right\}, \quad T_i^* = \exp \left\{ -\frac{Z_i^{*2}}{2(1+h^2)} \right\}.$$

We first notice that V_i is constructed to always satisfy $\widehat{\mu}_{D,i}^{EB} \geq V_{2i}$ (see the derivation of (35)), and $\widehat{\mu}_{D,i}^{EB} \geq V_{1i}$ on $E = \cap_{i=1}^{p_1} E_i$. E is the set of events in which Z_i s satisfy a specific relationship, with $P(E) \rightarrow 1$ as $p \rightarrow \infty$. Here, we defer the detailed definition of E to Appendix B. This implies that $\widehat{\mu}_{D,i}^{EB}$ can be bounded by V_{1i} with large probability and otherwise, by V_{2i} .

- In addition, one can rewrite V_{1i} as

$$V_{1i} = \frac{h^2 Z_i^*}{1+h^2} + \frac{\frac{1}{\sqrt{2\pi}} \left(\frac{h^2 Z_i^*}{1+h^2} + \frac{h(p_1-1)a_n \Delta T_i}{(1+h^2)^{3/2}} \right) - 2p^{1/2+\epsilon} \left(\frac{h^2 Z_i^*}{1+h^2} + \frac{1}{h^2} \right)}{\frac{1}{\sqrt{2\pi}} + \frac{1}{\sqrt{2\pi}} \frac{h \{(p_1-1)T_i + (p-p_1)T_i^*\}}{(1+h^2)^{1/2}} - 2p^{1/2+\epsilon}}$$

By plugging in the inequality $|Z_i| + a_n \Delta \leq \sqrt{2\alpha(\log p + 1)}$ in V_{1i} and the condition from E_{5i} for V_{2i} , we obtain $W_i \leq V_i$ for W_i defined above.

Eventually, W_i serves as the lower bound of $\widehat{\mu}_{D,i}^{EB}$ which are mutually independent. Therefore, by applying WLLN for triangular arrays on W_i , we show the second inequality of the lemma.

For large enough p which satisfies

$$\log p \geq \sqrt{2\alpha(\log p + 1)}, \quad (26)$$

$$|W_{1i}| \leq \frac{h^2}{1+h^2} \left\{ \log p + \frac{(1 + 2\sqrt{2\pi}p^{1/2+\epsilon}) \log p + (1+h^2)/h^4}{p^{1-\alpha}(1-p^{a-1}) - 2p^{1/2+\epsilon}} \right\}$$

and

$$|W_{2i}| \leq \Delta + 2(\log p)^2/a_n$$

holds on E since $\max_{1 \leq i \leq n} |Z_i| < \log p$ and $1/h^2 = \log p$. Therefore,

$$|W_i| \leq 1 + 2(\log p)^2/a_n.$$

In addition, from (26), one can obtain

$$\begin{aligned} E[W_1] &= E \left[W_{1i} \mid |Z_i| + a_n \Delta \leq \sqrt{2\alpha(\log p + 1)} \right] \times P \left(|Z_i| + a_n \Delta \leq \sqrt{2\alpha(\log p + 1)} \right) \\ &\quad + E \left[W_{2i} \mid |Z_i| + a_n \Delta > \sqrt{2\alpha(\log p + 1)} \right] \times P \left(|Z_i| + a_n \Delta > \sqrt{2\alpha(\log p + 1)} \right) \\ &> \left\{ \frac{h^2}{1 + h^2} a_n \Delta - \frac{1 + 2\sqrt{2\pi} p^{1/2+\epsilon} + \log p}{p^{1-\alpha}(1 - p^{a-1}) - 2p^{1/2+\epsilon}} \right\} (1 - \gamma) + \left(\Delta - \frac{1}{a_n h^2} \log p \right) \gamma, \end{aligned}$$

where we define $\gamma = P \left(|Z_i| + a_n \Delta > \sqrt{2\alpha(\log p + 1)} \right)$. Note that

$$E \left[Z_i \mid |Z_i| < c \right] = 0.$$

By applying lemma 3 and comparing the order of p in each term, one can obtain that for b which satisfy $b > \alpha + \epsilon - 1/2$ and $b > -\alpha$,

$$E[W_1] \geq \frac{h^2}{1 + h^2} a_n \Delta \{1 + o(1)\}$$

holds. Note that when $b > -1/4$, in which all $(a, b) \in \mathcal{R}_{NPEB}$ with $b < 0$ are included, we can always pick such $\alpha, \epsilon > 0$ as $\epsilon = b + 1/4$, $\alpha = 1/4$. From the WLLN for triangular arrays,

$$\frac{\sum_{i=1}^{p_1} W_i - p_1 E[W_1]}{1 + 2(\log p)^2/a_n} \xrightarrow{P} 0. \quad (27)$$

Therefore, one can write

$$\sum_{i=1}^{p_1} W_i \geq \frac{h^2}{1+h^2} a_n p^{a+b} \{1 + o(1)\} + o_p \{(\log p)^2\}.$$

□

B Proof of Theorem 1

We define $\bar{z}_D = \bar{z}_1 - \bar{z}_2$ which has $\bar{z}_D \sim N(\mu_D^*, a_n^{-2} I_p)$ where $a_n = (1/n_1 + 1/n_2)^{-1/2}$. From (13), the estimator using EB method of mean difference μ_D^* is as follows:

$$\widehat{\mu}_{D,i}^{EB} = \bar{z}_{D,i} + \frac{1}{h^2} \frac{\sum_{j=1}^p (\bar{z}_{D,j} - \bar{z}_{D,i}) \phi \left\{ \frac{a_n (\bar{z}_{D,i} - \bar{z}_{D,j})}{h} \right\}}{\sum_{j=1}^p \phi \left\{ \frac{a_n (\bar{z}_{D,i} - \bar{z}_{D,j})}{h} \right\}}. \quad (28)$$

Here, $\widehat{\mu}_{D,i}^{EB}$, $\bar{z}_{D,i}$ denotes the i -th component of the EB estimator of the mean vector $\widehat{\mu}_D^{EB}$ and \bar{z}_D , respectively. $\phi(\cdot)$ is the probability distribution function of standard Gaussian distribution. According to [3] and [10], we choose the bandwidth $h = 1/\sqrt{\log p}$ in (28).

Since $\bar{z}_D \sim N(\mu_D^*, a_n^{-2} I_p)$, we have $\bar{z}_{D,i} \sim N(\mu_i^*, a_n^{-2})$ which are mutually independent. Thus, we can rewrite $\bar{z}_{D,i}$ as follows using independent $Z_i \sim N(0, 1)$ for $1 \leq i \leq p$:

$$\bar{z}_{D,i} = \begin{cases} \Delta + Z_i/a_n, & \text{if } 1 \leq i \leq p_1 \\ Z_i/a_n, & \text{if } p_1 + 1 \leq i \leq p. \end{cases}$$

For simplicity in expressions, we define the followings, aligned with lemma 4 :

$$Z_{ij}^- = Z_i - Z_j, \quad Z_i^* = Z_i + a_n \Delta, \quad (29)$$

$$T_i = \exp \left\{ -\frac{Z_i^2}{2(1+h^2)} \right\}, \quad T_i^* = \exp \left\{ -\frac{Z_i^{*2}}{2(1+h^2)} \right\}. \quad (30)$$

With these notations, $\widehat{\mu}_{D,i}^{EB}$ is represented as

$$\widehat{\mu}_{D,i}^{EB} = \begin{cases} \Delta + \frac{Z_i}{a_n} + \frac{\sum_{j=1}^{p_1} \frac{Z_{ji}^-}{a_n} \phi(Z_{ij}^-/h) + \sum_{j=p_1+1}^p \frac{Z_{ji}^- - a_n \Delta}{a_n} \phi\{(Z_{ij}^- + a_n \Delta)/h\}}{h^2 \left[\sum_{j=1}^{p_1} \phi(Z_{ij}^-/h) + \sum_{j=p_1+1}^p \phi\{(Z_{ij}^- + a_n \Delta)/h\} \right]}, & \text{if } 1 \leq i \leq p_1 \\ \frac{Z_i}{a_n} + \frac{\sum_{j=1}^{p_1} \frac{Z_{ji}^- + a_n \Delta}{a_n} \phi\{(Z_{ij}^- - a_n \Delta)/h\} + \sum_{j=p_1+1}^p \frac{Z_{ji}^-}{a_n} \phi(Z_{ij}^-/h)}{h^2 \left[\sum_{j=1}^{p_1} \phi\{(Z_{ij}^- - a_n \Delta)/h\} + \sum_{j=p_1+1}^p \phi(Z_{ij}^-/h) \right]}, & \text{if } p_1 + 1 \leq i \leq p \end{cases} \quad (31)$$

We now show that, for $(a, b) \in A \cup C \cup D$, we have the divergence of V to ∞ in probability as in (18).

For this, we consider two cases depending on the sign of b : (i) $b < 0$ for $(a, b) \in A \cup D$ and (ii) $b > 0$ for $(a, b) \in C$. First, we show that among the region that satisfies $b < 0$, the region $A \cup D$ is a subset of \mathcal{R}_{NPEB} .

Claim I: $A \cup D \subset \mathcal{R}_{NPEB}$

In this case, we provide the proof of $\mathcal{R}_{NPEB} \supset A \cup D$, in which (a, b) satisfies $a + 2b > 0$ and $-1/4 < b < 0$. For the proof of (18), we have the following roadmap consisting of two steps :

Step 1 : We present a lower bound of the numerator in V such as

$$\widehat{\mu}_D^* \mu_D^* \geq \frac{h^2}{1 + h^2} a_n p^{a+2b} \{1 + o_p(1)\}.$$

Step 2 : We then propose an upper bound of the denominator in V as

$$\|\widehat{\mu}_D^*\|_2 = O_p \left\{ p^{\max(2a+2b-1, \epsilon')} \right\},$$

where ϵ' is an arbitrary positive constant.

We present the proofs of (i) Step 1 and (ii) Step 2 as follows.

- *Proof of Step 1:* From the expression of $\widehat{\mu}_{D,i}^{EB}$ in (31), one can observe that

$$\widehat{\mu}_{D,i}^{EB} \equiv \Delta + \frac{Z_i}{a_n} + \frac{1}{h^2} \left(\sum_{j=1}^{p_1} w_j \frac{Z_{ji}^-}{a_n} + \sum_{j=p_1+1}^p w_j \frac{Z_{ji}^- - a_n \Delta}{a_n} \right) \quad (32)$$

for $1 \leq i \leq p_1$, where $\sum_{j=1}^p w_j = 1$ with

$$w_j = \phi(Z_{ij}^-/h) \left/ \left[\sum_{j=1}^{p_1} \phi(Z_{ij}^-/h) + \sum_{j=p_1+1}^p \phi\{(Z_{ij}^- + a_n \Delta)/h\} \right] \right. \quad (33)$$

for $1 \leq j \leq p_1$ and

$$w_j = \phi\{(Z_{ij}^- + a_n \Delta)/h\} \left/ \left[\sum_{j=1}^{p_1} \phi(Z_{ij}^-/h) + \sum_{j=p_1+1}^p \phi\{(Z_{ij}^- + a_n \Delta)/h\} \right] \right. \quad (34)$$

for $p_1 + 1 \leq j \leq p$. From (32), one can check that

$$\widehat{\mu}_{D,i}^{EB} \geq \Delta + \frac{Z_i}{a_n} + \frac{1}{a_n h^2} \min \{(Z_{ji}^-)_{1 \leq j \leq p_1}, (Z_{ji}^- + a_n \Delta)_{p_1+1 \leq j \leq p}\} \quad (35)$$

always holds for $1 \leq i \leq p_1$ since the weighted mean is always greater than the minimum value.

Subsequently, we define A_i, B_i, C_i, D_i as follows:

$$\begin{aligned} A_i &= \sum_{j=1}^{p_1} \frac{Z_{ji}^-}{a_n} \phi(Z_{ij}^-/h) \equiv \sum_{j=1}^{p_1} w_{1j} \frac{Z_{ji}^-}{a_n}, \\ B_i &= \sum_{j=p_1+1}^p \phi\{(Z_{ij}^- + a_n \Delta)/h\} \frac{Z_{ji}^- - a_n \Delta}{a_n} \equiv \sum_{j=1}^{p_1} w_{2j} \frac{Z_{ji}^- - a_n \Delta}{a_n}, \end{aligned}$$

$$C_i = \sum_{j=1}^{p_1} \phi(Z_{ij}^-/h) \equiv \sum_{j=1}^{p_1} w_{1j},$$

$$D_i = \sum_{j=p_1+1}^p \phi\{(Z_{ij}^- + a_n\Delta)/h\} \equiv \sum_{j=p_1+1}^p w_{2j}.$$

For Z_i and Z_j ($i \neq j$), one can check

$$E \left[\phi(Z_{ji}^-/h) \middle| Z_i \right] = \frac{h}{\sqrt{2\pi}\sqrt{1+h^2}} T_i,$$

$$E \left[Z_{ij}^- \phi(Z_{ji}^-/h) \middle| Z_i \right] = -\frac{h^3}{\sqrt{2\pi}\sqrt{1+h^2}^3} Z_i T_i$$

by direct calculation. A similar relation holds for Z_i^* and T_i^* as follows.

$$E \left[\phi\{(Z_{ji}^- - a_n\Delta)/h\} \middle| Z_i^* \right] = \frac{h}{\sqrt{2\pi}\sqrt{1+h^2}} T_i^*,$$

$$E \left[(Z_{ij}^- + a_n\Delta) \phi\{(Z_{ji}^- - a_n\Delta)/h\} \middle| Z_i^* \right] = -\frac{h^3}{\sqrt{2\pi}\sqrt{1+h^2}^3} Z_i^* T_i^*.$$

In addition, using the fact that $\phi(x) \in (0, 1/\sqrt{2\pi}]$, we obtain the following result : for $1 \leq i \leq p_1$, Z_{ij}^- are conditionally independent on Z_i , for all $j \neq i$. Therefore, for every $\epsilon > 0$, by Hoeffding's inequality, we have

$$P \left(\left| C_i - \frac{1}{\sqrt{2\pi}} - \frac{(p_1-1)h}{\sqrt{2\pi}\sqrt{1+h^2}} T_i \right| > p_1^{1/2+\epsilon} \middle| Z_i \right) \leq 2 \exp(-4\pi(p_1-1)^{2\epsilon}) \quad (36)$$

since

$$E [C_i | Z_i] = E \left[\sum_{j=1}^{p_1} \phi(Z_{ij}^-/h) \middle| Z_i \right] = \frac{1}{\sqrt{2\pi}} + \frac{(p_1-1)h}{\sqrt{2\pi}\sqrt{1+h^2}} T_i.$$

By taking the expectation of Z_i in (36), we have

$$P \left(\left| C_i - \frac{1}{\sqrt{2\pi}} - \frac{(p_1-1)h}{\sqrt{2\pi}\sqrt{1+h^2}} T_i \right| > p_1^{1/2+\epsilon} \right) \leq 2 \exp \{ -4\pi(p_1-1)^{2\epsilon} \}. \quad (37)$$

Similarly, we also have

$$P \left(\left| D_i - \frac{(p-p_1)h}{\sqrt{2\pi}\sqrt{1+h^2}} T_i^* \right| > (p-p_1)^{1/2+\epsilon} \right) \leq 2 \exp \{ -4\pi(p-p_1)^{2\epsilon} \}. \quad (38)$$

Also, from $|x\phi(x)| \leq 1/\sqrt{2\pi e}$, we obtain

$$P \left(\left| A_i + \frac{(p_1-1)h^3 Z_i}{\sqrt{2\pi}\sqrt{1+h^2}^3} T_i \right| > p_1^{1/2+\epsilon} \right) \leq 2 \exp \{ -\pi e (p_1-1)^{2\epsilon} \log p \},$$

$$P \left(\left| B_i + \frac{(p-p_1)h^3 Z_i^*}{\sqrt{2\pi}\sqrt{1+h^2}^3} T_i^* \right| > (p-p_1)^{1/2+\epsilon} \right) \leq 2 \exp \{ -\pi e (p-p_1)^{2\epsilon} \log p \}.$$

Now, we define the events E_{1i}, \dots, E_{5i} as follows:

$$E_{1i} = \left\{ \left| A_i + \frac{(p_1-1)h^3 Z_i}{\sqrt{2\pi}\sqrt{1+h^2}^3} T_i \right| < p_1^{1/2+\epsilon} \right\},$$

$$E_{2i} = \left\{ \left| B_i + \frac{(p-p_1)h^3 Z_i^*}{\sqrt{2\pi}\sqrt{1+h^2}^3} T_i^* \right| < (p-p_1)^{1/2+\epsilon} \right\},$$

$$E_{3i} = \left\{ \left| C_i - \frac{1}{\sqrt{2\pi}} - \frac{(p_1-1)h}{\sqrt{2\pi}\sqrt{1+h^2}} T_i \right| < p_1^{1/2+\epsilon} \right\},$$

$$E_{4i} = \left\{ \left| D_i - \frac{(p-p_1)h}{\sqrt{2\pi}\sqrt{1+h^2}} T_i^* \right| < (p-p_1)^{1/2+\epsilon} \right\},$$

$$E_{5i} = \left\{ \max_{1 \leq j \leq p} |Z_j| + a_n \Delta < \log p \right\}.$$

Let $E_i = \bigcap_{j=1}^5 E_{ji}$. Applying Bonferroni's inequality on E_i^c and from Lemma 2, we obtain

$$\begin{aligned} P(E_i) &= 1 - P(E_i^c) = 1 - P(\bigcup_{j=1}^5 E_{ji}^c) \\ &\geq 1 - \sum_{j=1}^5 P(E_{ji}^c) \\ &= 1 - 8 \exp \{ -\pi e (p_1-1)^{2\epsilon} \} - 1/p. \end{aligned}$$

Therefore, when we define $E = \cap_{i=1}^{p_1} E_i$, we have

$$\begin{aligned}
P(E) &= 1 - P(E^c) = 1 - P(\cup_{i=1}^{p_1} E_i^c) \\
&\geq 1 - \sum_{i=1}^{p_1} \{1 - P(E_i)\} \\
&\geq 1 - 8p_1 \exp\{-\pi e(p_1 - 1)^{2\epsilon}\} - 1/p^{1-a}
\end{aligned} \tag{39}$$

Note that for all $0 < a < 1$, $\lim_{p \rightarrow \infty} P(E) = 1$. On the event E , we can set the bounds for A_i, B_i, C_i, D_i to eventually build a lower bound of $\widehat{\mu}_{D,i}^{EB}$. Since $\lim_{p \rightarrow \infty} P(E) = 1$, our aim is to define an appropriate lower bound, W_i , on E which satisfies

$$V = \frac{\widehat{\mu}_D^{*T} \mu_D^*}{\|\widehat{\mu}_D^*\|_2} = \frac{\Delta \sum_{i=1}^{p_1} \widehat{\mu}_{D,i}^{EB}}{\|\widehat{\mu}_D^*\|_2} \geq \frac{\Delta \sum_{i=1}^{p_1} W_i}{\|\widehat{\mu}_D^*\|_2} \xrightarrow{p} \infty. \tag{40}$$

for $(a, b) \in \mathcal{R}_{NPEB}$.

We directly apply the result in Lemma 4 and obtain $\Delta \sum_{i=1}^{p_1} \widehat{\mu}_{D,i}^{EB} \geq \Delta \sum_{i=1}^{p_1} W_i$ where W_i is defined in Lemma 4 which leads to

$$\widehat{\mu}_D^{*T} \mu_D^* = \Delta \sum_{i=1}^{p_1} \widehat{\mu}_{D,i}^{EB} \geq \Delta \sum_{i=1}^{p_1} W_i \geq \frac{h^2}{1 + h^2} a_n p^{a+2b} \{1 + o_p(1)\}. \tag{41}$$

This inequality holds on E , and E has the probability larger than

$$1 - 8p_1 \exp\{-\pi e(p_1 - 1)^{2\epsilon}\} - p^{-1+a},$$

which goes to 1 for all $0 < a < 1$ as $p \rightarrow \infty$.

• *Proof of Step 2:* The denominator in (18) can be bounded using the equation (45) in [3].

For $\nu = 1 + h^2$, let

$$\begin{aligned}
\delta_i &:= \frac{\sum_{j=1}^{p_1} \Delta \phi \{(a_n \bar{z}_{D,i} - a_n \Delta) / \sqrt{\nu}\}}{\sum_{j=1}^{p_1} \phi \{(a_n \bar{z}_{D,i} - a_n \Delta) / \sqrt{\nu}\} + \sum_{j=p_1+1}^p \phi (a_n \bar{z}_{D,i} / \sqrt{\nu})} \\
&= \begin{cases} \frac{p_1 \Delta \phi (Z_i / \sqrt{\nu})}{p_1 \phi (Z_i / \sqrt{\nu}) + (p - p_1) \phi \{(a_n \Delta + Z_i) / \sqrt{\nu}\}}, & \text{if } 1 \leq i \leq p_1 \\ \frac{p_1 \Delta \phi \{(Z_i - a_n \Delta) / \sqrt{\nu}\}}{p_1 \phi \{(Z_i - a_n \Delta) / \sqrt{\nu}\} + (p - p_1) \phi (Z_i / \sqrt{\nu})}, & \text{if } p_1 + 1 \leq i \leq p \end{cases}.
\end{aligned}$$

Then the equation (45) in [3] implies

$$E \left[\sum_{i=1}^p (\delta_i - \widehat{\mu}_{D,i}^{EB})^2 \right] = o(p^\epsilon) \quad (42)$$

for all $\epsilon > 0$. Using this, one obtain the probabilistic upper bound of $\|\widehat{\mu}_D^{EB}\|_2^2$ from

$$\|\widehat{\mu}_D^{EB}\|_2^2 \leq 2 \sum_{i=1}^p (\delta_i - \widehat{\mu}_{D,i}^{EB})^2 + 2 \sum_{i=1}^p \delta_i^2. \quad (43)$$

Since Z_i are i.i.d., $E \left[\sum_{i=1}^p \delta_i^2 \right]$ is simplified as follows :

$$\begin{aligned}
E \left[\sum_{i=1}^p \delta_i^2 \right] &= p_1 E \left[\frac{p_1 \Delta \phi (Z_i / \sqrt{\nu})}{p_1 \phi (Z_i / \sqrt{\nu}) + (p - p_1) \phi \{(a_n \Delta + Z_i) / \sqrt{\nu}\}} \right]^2 \\
&\quad + (p - p_1) E \left[\frac{p_1 \Delta \phi \{(Z_i - a_n \Delta) / \sqrt{\nu}\}}{p_1 \phi \{(Z_i - a_n \Delta) / \sqrt{\nu}\} + (p - p_1) \phi (Z_i / \sqrt{\nu})} \right]^2 \\
&= p_1 E \left[\frac{p_1 \Delta}{p_1 + (p - p_1) \exp \{-a_n \Delta (a_n \Delta + 2Z_i) / (2\nu)\}} \right]^2 \\
&\quad + (p - p_1) E \left[\frac{p_1 \Delta \exp \{-a_n \Delta (a_n \Delta - 2Z_i) / (2\nu)\}}{p_1 \exp [-a_n \Delta (a_n \Delta - 2Z_i) / (2\nu)] + (p - p_1)} \right]^2
\end{aligned}$$

$$=: J_1 + J_2.$$

From $e^{-x} \geq 1 - x$ for all x , under the event E , J_1 and J_2 satisfy

$$J_1 \leq p_1 \left\{ \frac{p_1 \Delta}{p - (p - p_1) a_n \Delta (a_n \Delta + 2 \log p) / 2} \right\}^2, \quad J_2 \leq (p - p_1) \left\{ \frac{p_1 \Delta}{p_1 + (p - p_1)} \right\}^2,$$

which implies $E[\sum_{i=1}^p \delta_i^2] \leq p^{2a+2b-1} \{1 + o(1)\}$. As a result, from (42) and (43), we have

$$\|\widehat{\mu}_D^{EB}\|_2^2 = O_p \left\{ p^{\max(2a+2b-1, \epsilon')} \right\} \quad (44)$$

for all $\epsilon' > 0$.

Therefore, we prove the results in *Step 1* and *Step 2* leading to

$$\begin{aligned} V &= \frac{\widehat{\mu}_D^{*T} \mu_D^*}{\|\widehat{\mu}_D^*\|_2} \geq \frac{h^2}{1 + h^2} \frac{a_n p^{a+2b} (1 + o_p(1))}{\sqrt{p^{\max(2a+2b-1, \epsilon')} O_p(1)}} \\ &= \frac{a_n}{\log p} p^{a+2b - \max(a+b-1/2, \epsilon'/2)} \frac{1 + o_p(1)}{\sqrt{O_p(1)}} \xrightarrow{P} \infty \end{aligned}$$

for $-1/4 < b < 0$ and $a + 2b > \epsilon'/2$ since $a + 2b - \max(a + b - 1/2, \epsilon'/2) > 0$ for the given region of (a, b) .

Subsequently, we show that the region C is a subset of \mathcal{R}_{NPEB} among the region that satisfies $b > 0$.

Claim II: $C \subset \mathcal{R}_{NPEB}$

Here, we show (18) is satisfied for all $(a, b) \in C$ under the NPEB method. Since $\widehat{\mu}_D^{*T} \mu_D^* = \Delta \sum_{i=1}^{p_1} \widehat{\mu}_{D,i}^{EB}$ and $\widehat{\mu}_{D,i}^{EB} \geq V_{2i}$ always holds,

$$\widehat{\mu}_D^*{}^T \mu_D^* \geq \Delta \left(\sum_{i=1}^{p_1} \left[\Delta + \frac{1}{a_n} Z_i + \frac{1}{a_n h^2} \min \{ (Z_{ji}^-)_{1 \leq j \leq p_1}, (Z_{ji}^- + a_n \Delta)_{p_1+1 \leq j \leq p} \} \right] \right) \quad (45)$$

$$\geq \Delta \left[\sum_{i=1}^{p_1} \left\{ \Delta + \left(\frac{1}{a_n} - \frac{1}{a_n h^2} \right) Z_i - \frac{1}{a_n h^2} \min_{1 \leq j \leq p} Z_j \right\} \right]. \quad (46)$$

Therefore, from Lemma 2 and the WLLN, one can obtain $\widehat{\mu}_D^*{}^T \mu_D^* \geq p^{a+2b} \{1 + o_p(1)\}$.

In addition, by using $E[\exp(cZ_i)] = \exp(c^2/2)$ for any constant $c > 0$, we have

$$\begin{aligned} E \sum_{i=1}^p \delta_i^2 &\leq p_1 \Delta^2 + (p - p_1) E \left[\frac{p_1 \Delta \exp \{ -a_n \Delta (a_n \Delta - 2Z_i) / (2\nu) \}}{p - p_1} \right]^2 \\ &\leq p^{a+2b} + \frac{p^{2a+2b}}{p - p_1} = p^{a+2b} + p^{2a+2b-1} (1 + o(1)) \\ &= p^{a+2b} (1 + o(1)) \end{aligned}$$

where the last equality is from $a < 1$. Therefore, from (42) and (43), we obtain

$$\|\widehat{\mu}_D^*\|_2^2 = O_p(p^{a+2b}). \quad (47)$$

leading to

$$V = \frac{\widehat{\mu}_D^*{}^T \mu_D^*}{\|\widehat{\mu}_D^*\|_2} \geq \frac{p^{a+2b} \{1 + o_p(1)\}}{O_p\{p^{(a+2b)/2}\}} \xrightarrow{p} \infty$$

for all $a, b > 0$.

Therefore, our main Theorem 1 is proved by Claims I and II. \square